

Supporting Information

A Computational Study of Activation of Allenoates by Lewis Bases and Reactivity of Intermediate Adducts

Gou-Tao Huang, Timm Lankau, and Chin-Hui Yu*

*Department of Chemistry, National Tsing Hua University, 101, Section 2, Kuang-Fu Road,
HsinChu 30013, Taiwan*

E-mail: chyu@oxygen.chem.nthu.edu.tw

Contents

1 Assessment of performance of M06-2X	5
2 Addition of Lewis bases to <i>s-trans</i> methyl allenate	7
3 Electrostatic potential surface maps for the addition of LBs to <i>s-cis</i> 1	8
4 Solvent effect	12
5 Protonation and nucleophilicity	14
6 [3 + 2] cycloadditions with ethylene 2a	17

*To whom correspondence should be addressed

7 Cycloadditions with enone 2b	18
8 Cycloadditions with ketone 2c	22
9 Cartesian coordinates of optimized structures	27
9.1 LBs and methyl allenolate	27
9.2 Addition of LBs to <i>s-cis</i> methyl allenolate	29
9.2.1 Z-type addition	29
9.2.2 E-type addition	32
9.3 Proton affinity and methylation	35
9.3.1 Protonated Z-type adducts	35
9.3.2 Transition structures for the attack of the Z-type adducts on MeCl	38
9.4 [3 + 2] cycloaddition with ethylene 2a	41
9.5 [3 + 2] and [2 + 4] cycloadditions with enone 2b	44
9.5.1 Cycloadditions starting from Pph-3'	44
9.5.2 Cycloadditions starting from Dabco-3'	46
9.6 [2 + 2], [3 + 2] and [2 + 2 + 2] cycloadditions with ketone 2c	47
9.6.1 Cycloadditions starting from IPr-3'	47
9.6.2 Cycloadditions starting from Dabco-3'	51
9.6.3 Cycloadditions starting from Pph-3	53

List of Figures

S1 Evaluation of the M06-2X and CCSD(T) methods for the addition of PMe ₃ to methyl allenolate. The electronic energies, ΔE_{ele} in kcal mol ⁻¹ , are relative to separated reactants.	5
--	---

S2	Addition of pyridine (Py), 1,3-dimethylimidazolin-2-ylidene (IMe) and DABCO (Dabco) to methyl allenate calculated at the M06-2X and CCSD(T) levels. The electronic energies, ΔE_{ele} in kcal mol ⁻¹ , are relative to separated reactants.	6
S3	Addition of the Lewis base to <i>s-trans</i> methyl allenate. LB- ts3x and LB- 3x are the Z-type structures, and LB- ts3x' and LB- 3x' are the E-type structures.	7
S4	Z/E-type transition structures (LB- ts3 /LB- ts3') and adducts (LB- 3 /LB- 3') for the addition of Pph and Hmpt to <i>s-cis</i> 1 . Electrostatic potential is mapped onto the total electron density with the isosurface of 0.02.	9
S5	Z/E-type transition structures (LB- ts3 /LB- ts3') and adducts (LB- 3 /LB- 3') for the addition of Dabco to <i>s-cis</i> 1 . Electrostatic potential is mapped onto the total electron density with the isosurface of 0.02.	10
S6	Z/E-type transition structures (LB- ts3 /LB- ts3') and adducts (LB- 3 /LB- 3') for the addition of Dmap and Mtbd to <i>s-cis</i> 1 . Electrostatic potential is mapped onto the total electron density with the isosurface of 0.02.	11
S7	Protonation and methylation for the α - and γ -carbon atoms of the E-type adducts, LB- 3'	14
S8	Energy profiles for the PPh ₃ -catalyzed α - and γ -[3 + 2] cycloadditions.	18
S9	Energy profiles for the PPh ₃ -catalyzed γ -[3 + 2] and γ -[2 + 4] cycloadditions.	19
S10	Energy profiles for the PPh ₃ -catalyzed γ -[3 + 2] cycloadditions starting from Pph-3 and Pph-3'	20
S11	Energy profiles for the DABCO-catalyzed γ -[2 + 4] cycloadditions starting from Dabco-3 and Dabco-3'	21
S12	Energy profiles for the DABCO-catalyzed γ -[2 + 2], γ -[3 + 2] and γ -[2 + 2 + 2] cycloadditions of 1 and ketone 2c	22
S13	Energy profiles for the IPr -catalyzed γ -[2 + 2], γ -[3 + 2] and γ -[2 + 2 + 2] cycloadditions of 1 and ketone 2c	23

S14	Energy profiles for the IPr -catalyzed γ -[2 + 2 + 2] cycloadditions, yielding <i>trans</i> - and <i>cis</i> -products.	24
S15	Geometry of IPr-γ-5c'	25
S16	Energy profiles for the PPh_3 -catalyzed γ -[2 + 2], γ -[3 + 2] and γ -[2 + 2 + 2] cycloadditions of 1 and ketone 2c	26

List of Tables

S1	Free energies and enthalpies (ΔG [ΔH] in kcal mol ⁻¹) for the addition of the Lewis bases to <i>s-trans</i> 1 . All energies are relative to the separated Lewis bases and methyl allenolate 1	8
S2	Solvent effect on free energies and enthalpies (ΔG [ΔH] in kcal mol ⁻¹) for the addition of the four Lewis bases, IPr , Pph , Dabco and Dmap , to <i>s-cis</i> 1	12
S3	Computed dipole moments (unit in Debye) for the transition states and adducts in five different solvents.	13
S4	Proton affinities calculated according to the formula, $\Delta H = (H_{\text{LB-3}'}^{298} + H_{\text{proton}}^{298}) - H_{\text{LB-3'-H}}^{298}$ where $\Delta H_{\text{proton}}^{298}$ is equal to 1.5 kcal mol ⁻¹ . The activation free energies, ΔG^\ddagger in kcal mol ⁻¹ , for the the $\text{S}_{\text{N}}2$ attack on MeCl are reported relative to the separated reactants, Lewis bases and allenotes.	15
S5	Hirshfeld atomic charges on the C_α and C_γ in LB-3 with and without summing the attached hydrogen atoms.	16
S6	HOMO-orbital contributions on the C_α and C_γ atoms in LB-3	16
S7	Free energies and enthalpies, ΔG [ΔH] in kcal mol ⁻¹ , for the [3 + 2] cycloaddition of the adducts (LB-3 and LB-3') and ethylene 2a	17

1 Assessment of performance of M06-2X

The reaction of trimethylphosphine with methyl allenate yielding the $\text{PMe}_3 \cdot$ allenate adduct is used to evaluate the accuracy of the chosen computational method (Figure S1). The M06-2X/6-31+G* method was used to optimize all geometries discussed in this paper. Additional single point calculations with the optimized geometries employing more sophisticated methods, M06-2X/6-311++G**, CCSD(T)/6-31+G* and CCSD(T)/6-311++G**, were done to obtain more reliable values for the electronic properties of the discussed structures. The M06-2X/6-311++G**//M06-2X/6-31+G* calculations show that the size of the basis set has only a small influence on the relative electronic energies of the discussed reaction (Figure S1). The range of energy difference is between 0.1 and 1.9 kcal mol⁻¹. The influence of the chosen correlation method is also small as the comparison of the M06-2X results with those obtained from CCSD(T) calculations shows. The M06-2X energies are up to 3 kcal mol⁻¹ lower than the CCSD(T) energies, but the two methods show the same chemical trend.

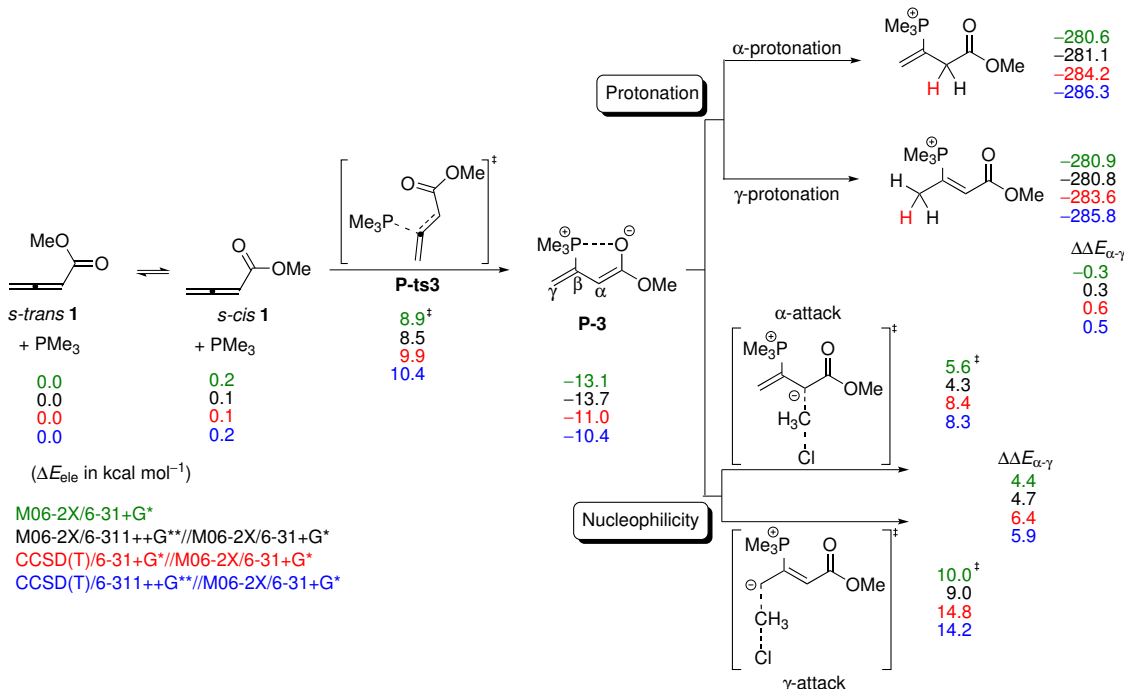


Figure S1: Evaluation of the M06-2X and CCSD(T) methods for the addition of PMe_3 to methyl allenate. The electronic energies, ΔE_{ele} in kcal mol⁻¹, are relative to separated reactants.

The α - and γ -carbon atoms in $\text{PMe}_3 \cdot$ allenolate have both basic and nucleophilic properties. The protonated α - and γ -adducts differ less than 1 kcal mol⁻¹ in energy, and hence the C_α and C_γ atoms have similar proton affinities (Figure S1). However, the barrier for the nucleophilic attack of C_α at the carbon atom of CH_3Cl is 4 to 5 kcal mol⁻¹ lower in energy than that for the corresponding reaction of C_γ , which indicates that C_α is significantly more nucleophilic than C_γ . The M06-2X data are qualitatively reproduced by the high level CCSD(T) calculations displaying the same reactivity.

Similar tests for the addition of the allenolate to pyridine (**Py**), 1,3-dimethylimidazolin-2-ylidene (**IMe**) and 1,4-diazabicyclo[2.2.2]octane (**Dabco**) (Figure S2) show that the CCSD(T) calculations essentially reproduce the M06-2X data with a maximum error of 3 kcal mol⁻¹ in ΔE_{ele} while predicting the same chemical reactivity. Hence, the less expensive M06-2X/6-31+G* method was used for calculations discussed in this study.

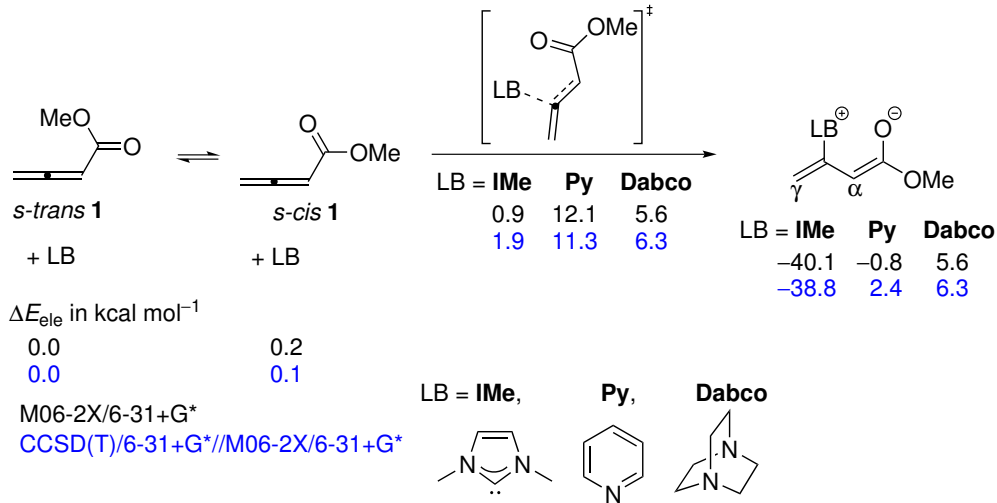


Figure S2: Addition of pyridine (**Py**), 1,3-dimethylimidazolin-2-ylidene (**IMe**) and DABCO (**Dabco**) to methyl allenolate calculated at the M06-2X and CCSD(T) levels. The electronic energies, ΔE_{ele} in kcal mol⁻¹, are relative to separated reactants.

2 Addition of Lewis bases to *s-trans* methyl allenolate **1**

Figure S3 shows the mechanism of the addition of the Lewis base to *s-trans* methyl allenolate **1**. Table S1 summarizes the barriers of the Z/E-type addition and the energies of the forming adducts. The addition to *s-trans* **1** is less favorable than that to *s-cis* **1** (Scheme 2 and Table 1 in the main text).

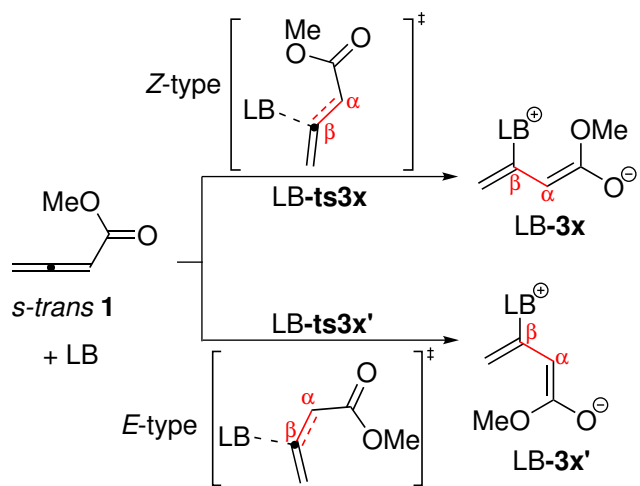


Figure S3: Addition of the Lewis base to *s-trans* methyl allenate. LB-**ts3x** and LB-**3x** are the Z-type structures, and LB-**ts3x'** and LB-**3x'** are the E-type structures.

	Z-type addition		E-type addition	
	LB- ts3x	LB- 3x	LB- ts3x'	LB- 3x'
LB = NHC				
IMe	17.3 [3.3]	-18.5 [-32.6]		
IPr	18.8 [3.8]	-14.4 [-30.7]	17.0 [1.1]	-14.0 [-28.7]
phosphine				
Pbu	22.8 [8.4]	9.6 [-6.8]		
Pph	26.0 [9.8]	16.6 [-1.2]	28.9 [13.1]	17.2 [2.4]
Hmpt	28.3 [14.1]	6.5 [-7.0]	29.1 [15.5]	9.8 [-3.9]
amine				
Quin	23.5 [9.6]	23.0 [7.7]	24.5 [10.2]	21.9 [7.1]
Dabco	24.0 [10.9]	23.4 [9.5]	24.0 [11.5]	22.5 [9.0]
aza-heterocycle				
Dmap	24.1 [11.0]	14.7 [0.4]	25.3 [12.6]	16.5 [2.7]
Py	25.5 [13.2]	18.9 [5.5]	28.6 [15.4]	22.3 [8.5]
Dbu	21.1 [7.3]	4.6 [-10.2]	22.5 [8.4]	8.5 [-5.8]
Mtbd	26.4 [11.6]	7.8 [-7.4]	22.7 [9.5]	12.3 [-1.6]

Table S1: Free energies and enthalpies (ΔG [ΔH] in kcal mol⁻¹) for the addition of the Lewis bases to *s-trans* **1**. All energies are relative to the separated Lewis bases and methyl allenolate **1**.

3 Electrostatic potential surface maps for the addition of LBs to *s-cis* **1**

Figure S4 shows electrostatic potential surface maps for the transition states (TSs) and the adducts in the addition of **Pph** and **Hmpt** to *s-cis* **1**. The P···O distance in the Z-type TSs is closer than that in the E-type TSs, which suggests stronger electrostatic interactions in the Z-type structures. The carbonyl oxygen atom rests on the top of the phenyl ring or the dimethylamino group in the E-type TSs, and interacts therefore less with the P atom.

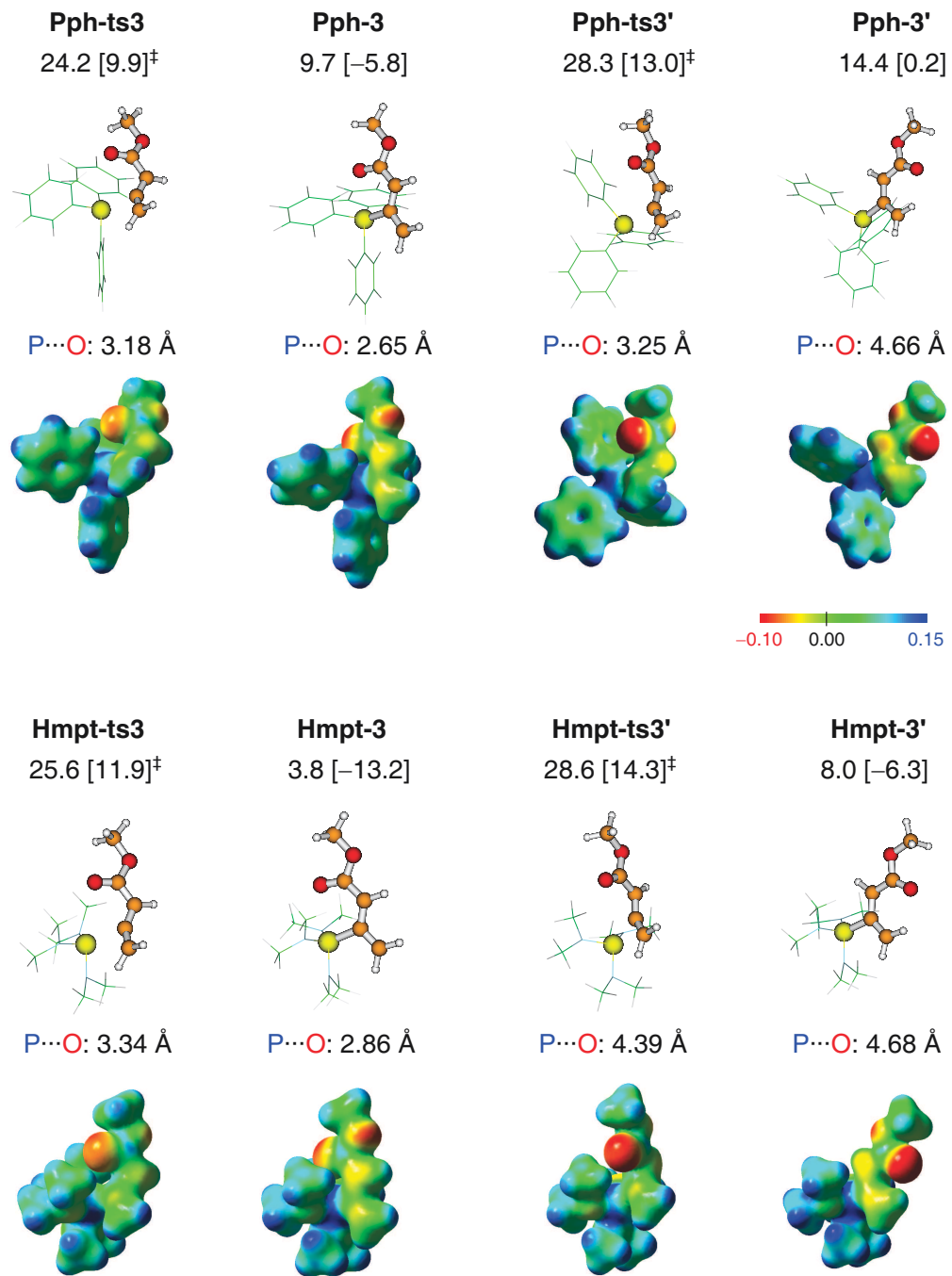


Figure S4: *Z/E*-type transition structures (LB-**ts3**/LB-**ts3'**) and adducts (LB-**3**/LB-**3'**) for the addition of **Pph** and **Hmpt** to *s-cis* **1**. Electrostatic potential is mapped onto the total electron density with the isosurface of 0.02.

The structures for the addition of **Dabco** to **1**, as shown in Figure S5, reveal that the carbonyl oxygen atom interacts with two methylene groups ($-\text{CH}_2-$) of **Dabco** in the Z-type addition, and with one methylene group in the E-type addition. The barrier for the rotation of the ester is 1.5 kcal mol⁻¹ higher than that for the the E-type addition of **Dabco** to the allenolate. The two-step addition process was also observed in the case of **Quin**. Hence, only the activation energies of the rate-determining TSs are listed for **Dabco** and **Quin** in Table 1 of the main text.

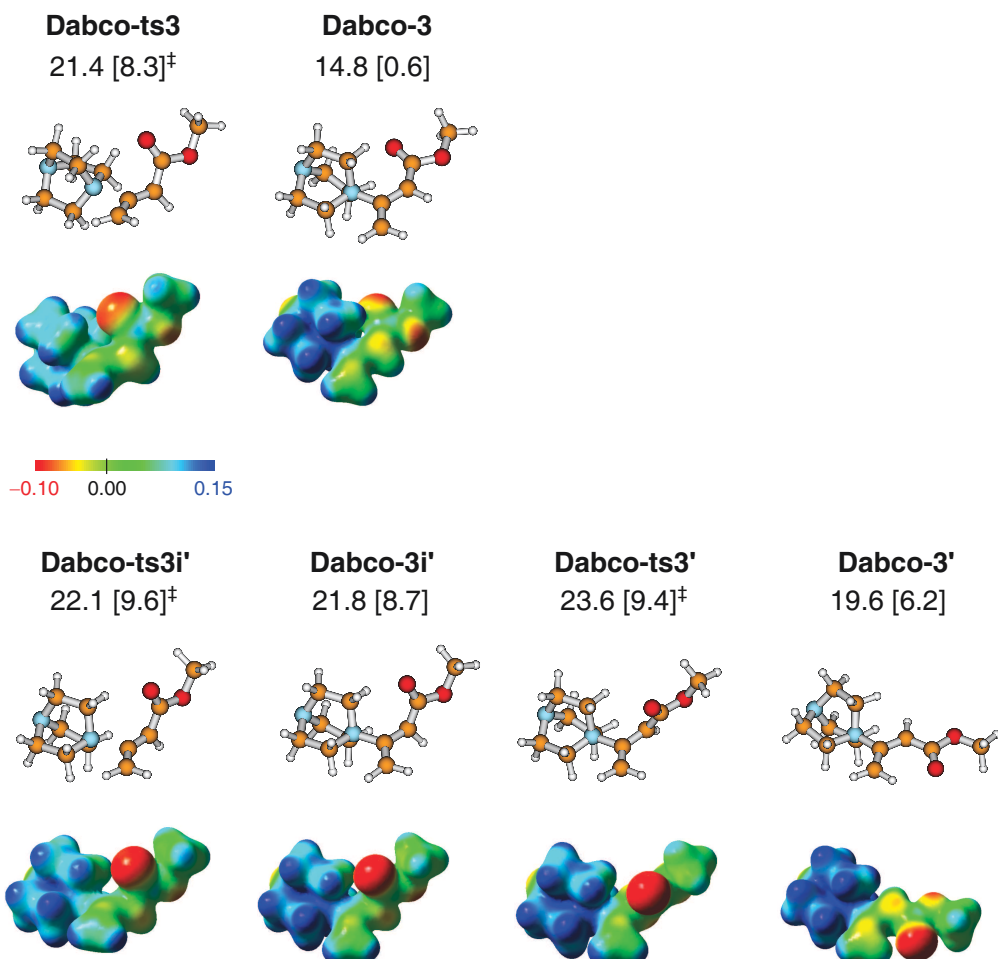


Figure S5: Z/E-type transition structures (LB-ts3/LB-ts3') and adducts (LB-3/LB-3') for the the addition of **Dabco** to *s-cis* **1**. Electrostatic potential is mapped onto the total electron density with the isosurface of 0.02.

Figure S6 shows geometries for the addition of **Dmap/Mtbs** to *s-cis* **1** and electrostatic potential surface maps. The carbonyl oxygen atom in **1** is oriented towards the pyridine ring in the Z-type structures (**Dmap-ts3** and **Dmap-3**), but points away from the pyridine ring in **Dmap-ts3'** and **Dmap-3'**. The carbonyl oxygen atom points towards the guanidine carbon atom in **Mtbd-ts3**, and towards the methyl group in **Mtbd-ts3'**. All of the Z-type TSs have favorable electrostatic interactions between the carbonyl oxygen atom and the LBs, stabilizing the structures.

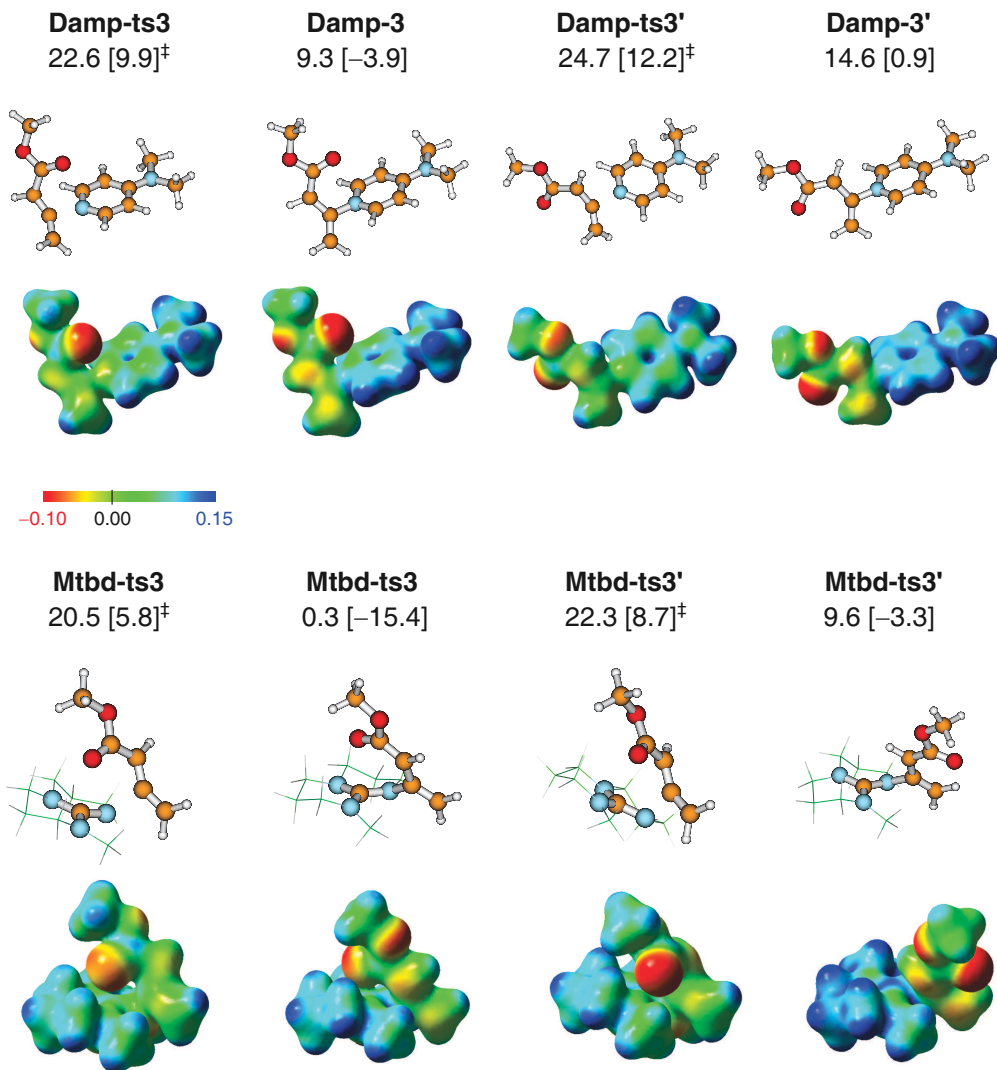


Figure S6: *Z/E*-type transition structures (LB-ts3/LB-ts3') and adducts (LB-3/LB-3') for the addition of **Dmap** and **Mtbd** to *s-cis* **1**. Electrostatic potential is mapped onto the total electron density with the isosurface of 0.02.

4 Solvent effect

Table S2 lists the free energies and enthalpies of selected stationary points in the addition of the four Lewis Bases, **IPr**, **Pph**, **Dabco** and **Dmap** to *s-cis* **1** in five different solvents. The computed dipole moments of the TSs and adducts optimized using the IEFPCM model are listed in Table S3. The dipole moment is larger in the *E*-type structures than that in the corresponding *Z*-type ones.

	vacuum $\epsilon = 1$	toluene 2.4	CHCl_3 4.7	THF 7.4	CH_2Cl_2 8.9	MeCN 35.7
IPr-ts3	17.7 [3.3]	19.2 [4.6]	19.7 [5.3]	20.4 [5.7]	20.5 [5.8]	20.4 [5.8]
IPr-ts3'	17.1 [2.3]	18.6 [3.1]	19.2 [3.6]	19.3 [3.8]	19.3 [3.6]	19.4 [4.3]
IPr-3	-21.3 [-36.3]	-20.7 [-36.3]	-21.0 [-36.4]	-20.7 [-36.5]	-20.6 [-36.6]	-20.3 [-36.6]
IPr-3'	-17.2 [-30.9]	-19.3 [-32.9]	-21.3 [-34.8]	-21.1 [-36.6]	-22.3 [-36.0]	-22.7 [-37.3]
Pph-ts3	24.2 [9.0]	24.6 [9.4]	24.4 [9.5]	24.2 [9.5]	22.8 [8.8]	22.8 [8.7]
Pph-ts3'	28.3 [13.0]	25.9 [11.8]	26.6 [11.2]	26.3 [10.8]	26.0 [10.7]	25.2 [10.2]
Pph-3	9.7 [-5.8]	8.8 [-6.5]	8.3 [-7.0]	8.2 [-7.3]	7.9 [-7.4]	7.6 [-7.9]
Pph-3'	14.4 [0.2]	11.5 [-3.1]	9.8 [-4.9]	9.1 [-5.7]	8.6 [-5.9]	7.5 [-7.0]
Dabco-ts3	21.4 [8.3]	21.6 [7.1]	19.6 [7.3]	19.6 [7.3]	19.6 [7.2]	19.1 [7.0]
Dabco-ts3'	23.6 [9.4]	21.8 [7.6]	18.3 [7.4]	19.1 [7.2]	19.0 [7.2]	18.7 [6.8]
Dabco-3	14.8 [0.6]	13.8 [-1.5]	11.6 [-1.9]	11.2 [-2.3]	11.0 [-2.4]	10.5 [-2.9]
Dabco-3'	19.6 [6.2]	15.3 [0.5]	11.5 [-1.5]	10.3 [-2.7]	10.0 [-3.0]	8.4 [-4.5]
Dmap-ts3	22.6 [9.9]	22.6 [9.9]	22.3 [9.7]	22.0 [9.6]	21.8 [9.5]	22.1 [9.3]
Dmap-ts3'	24.7 [12.2]	23.0 [10.5]	23.0 [10.5]	22.9 [10.3]	22.9 [10.3]	22.7 [10.0]
Dmap-3	9.3 [-3.9]	7.4 [-6.6]	6.2 [-8.0]	5.5 [-8.6]	5.3 [-8.8]	4.2 [-9.6]
Dmap-3'	14.6 [0.9]	9.2 [-4.6]	7.0 [-7.8]	5.2 [-8.3]	4.9 [-8.7]	3.6 [-10.0]

The stcutures with considering solvent effects were optimized in the IEFPCM model, rather than single-point caculations on the gas-optimized geometries.

Table S2: Solvent effect on free energies and enthalpies (ΔG [ΔH] in kcal mol⁻¹) for the addition of the four Lewis bases, **IPr**, **Pph**, **Dabco** and **Dmap**, to *s-cis* **1**.

	vacuum $\epsilon = 1$	toluene 2.4	CHCl_3 4.7	THF 7.4	CH_2Cl_2 8.9	MeCN 35.7
IPr-ts3	3.40	4.21	4.99	5.26	5.36	7.03
IPr-ts3'	4.89	5.74	6.37	6.61	6.68	7.40
IPr-3	6.26	7.57	8.44	8.91	9.06	9.73
IPr-3'	9.58	11.49	12.75	13.43	13.65	14.65
Pph-ts3	3.95	4.69	5.16	5.39	5.79	6.14
Pph-ts3'	5.71	6.44	6.91	7.05	7.09	7.31
Pph-3	5.73	7.03	7.82	8.20	8.33	8.87
Pph-3'	10.44	12.35	13.41	13.91	14.07	14.72
Dabco-ts3	3.97	4.59	4.87	5.04	5.10	5.34
Dabco-ts3'	5.46	5.67	5.71	5.72	5.82	8.72
Dabco-3	5.88	6.95	7.56	7.84	7.93	8.31
Dabco-3'	9.77	11.17	11.88	12.18	12.27	12.62
Dmap-ts3	7.11	8.24	8.70	8.90	9.29	9.59
Dmap-ts3'	10.53	11.13	11.40	11.51	11.55	11.71
Dmap-3	10.51	12.32	13.24	13.63	13.75	14.24
Dmap-3'	14.42	17.93	19.16	19.68	19.85	20.48

Table S3: Computed dipole moments (unit in Debye) for the transition states and adducts in five different solvents.

5 Protonation and nucleophilicity

Figure S7 shows the mechanism of α/γ -protonation of the *E*-type adducts LB-3' and the S_N2 reaction with CH_3Cl . Table S4 summarizes proton affinities and the barrier heights for the α/γ -attack of LB-3' on CH_3Cl . The C_γ atom usually has a higher proton affinity than C_α . However, the α -carbon is more nucleophilic than C_γ , as revealed by the lower barriers for the α -attack.

Tables S5 and S6 show the charges and the contributions of C_α and C_γ to the HOMO π -orbital in LB-3. Both the charges on and orbital coefficients of C_α are larger than those of C_γ .

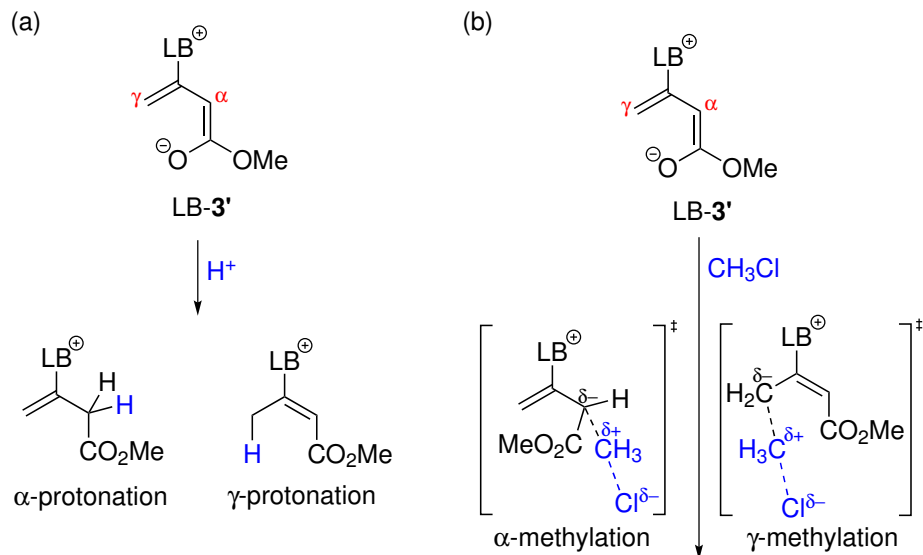


Figure S7: Protonation and methylation for the α - and γ -carbon atoms of the *E*-type adducts, LB-3'.

LB-3'	proton affinity (ΔH)		methylation (ΔG^\ddagger)	
	C _{α}	C _{γ}	C _{α}	C _{γ}
LB = NHC				
IMe	xx	xx	xx	xx
IPr	275.4	277.9	10.0	13.2
phosphine				
Pbu	xx	xx	xx	xx
Pph	270.4	271.0	42.8	45.9
Hmpt	268.3	268.4	36.1	39.5
amine				
Quin	266.9	266.6	49.0	52.1
Dabco	264.8	264.5	49.8	53.2
aza-heterocycle				
Dmap	266.7	269.9	41.7	45.2
Py	259.6	262.3	50.2	52.9
Dbu	275.5	273.2	33.8	36.5
Mtbd	275.1	277.7	34.7	41.1

Table S4: Proton affinities calculated according to the formula, $\Delta H = (H_{\text{LB-3'}}^{298} + H_{\text{proton}}^{298}) - H_{\text{LB-3'-H}}^{298}$ where $\Delta H_{\text{proton}}^{298}$ is equal to 1.5 kcal mol⁻¹. The activation free energies, ΔG^\ddagger in kcal mol⁻¹, for the the S_N2 attack on MeCl are reported relative to the separated reactants, Lewis bases and allenotes.

LB · allenolate	Hirshfeld charge with H		Hirshfeld charge without H	
	C _α	C _γ	C _α	C _γ
LB = NHC				
IMe	-0.15	-0.13	-0.18	-0.17
IPr	-0.14	-0.09	-0.17	-0.14
phosphine				
Pbu	-0.14	-0.09	-0.17	-0.14
Pph	-0.14	-0.08	-0.17	-0.14
Hmpt	-0.14	-0.09	-0.17	-0.14
amine				
Quin	-0.15	-0.11	-0.18	-0.17
Dabco	-0.15	-0.11	-0.18	-0.17
aza-heterocycle				
Dmap	-0.16	-0.14	-0.19	-0.18
Py	-0.16	-0.12	-0.18	-0.17
Dbu	-0.15	-0.14	-0.18	-0.17
Mtbd	-0.16	-0.12	-0.18	-0.17

Table S5: Hirshfeld atomic charges on the C_α and C_γ in LB-3 with and without summing the attached hydrogen atoms.

LB · allenolate	HOMO coefficient	
	C _α	C _γ
LB = NHC		
IMe	0.13	-0.10
IPr	0.13	-0.08
phosphine		
Pbu	0.14	-0.09
Pph	0.15	-0.10
Hmpt	0.14	-0.08
amine		
Quin	0.14	-0.09
Dabco	0.14	-0.09
aza-heterocycle		
Dmap	0.13	-0.09
Py	0.14	-0.09
Dbu	0.13	-0.09
Mtbd	0.13	-0.09

Table S6: HOMO-orbital contributions on the C_α and C_γ atoms in LB-3.

6 [3 + 2] cycloadditions with ethylene **2a**

The adducts, LB-**3** and LB-**3'**, react with ethylene **2a** to form five-membered rings with exocyclic C=C bonds or ylidic bonds. Free energies and enthalpies for the [3 + 2] cycloaddition are listed in Table S7. The formation of the [3+2] intermediates obtained with the NHCs, phosphines and aza-arenes is exergonic.

	[3+2] cycloaddition starting from LB- 3			[3+2] cycloaddition starting from LB- 3'		
	LB- 3 + 2a	LB- ts4a	LB- 4a	LB- 3' + 2a	LB- ts4a'	LB- 4a'
LB = NHC						
IMe	-23.3 [-38.0]	10.6 [-17.4]	-44.1 [-72.6]			
IPr	-21.3 [-36.3]	10.8 [-19.2]	-49.9 [-80.5]	-17.2 [-30.9]	9.9 [-19.1]	-52.1 [-82.5]
phosphine						
Pbu	1.4 [-13.9]	31.7 [3.6]	-12.9 [-40.2]			
Pph	9.7 [-5.8]	40.1 [11.2]	-6.6 [-36.5]	14.4 [0.2]	42.4 [14.5]	-8.5 [-39.3]
Hmpt	3.8 [-13.2]	33.1 [4.3]	-15.7 [-45.9]	8.0 [-6.3]	35.1 [7.9]	-15.4 [-44.1]
amine						
Quin	14.8 [-1.0]	49.0 [20.4]	13.4 [-16.3]	19.0 [4.2]	51.0 [22.5]	14.1 [-14.7]
Dabco	14.8 [0.6]	49.2 [22.1]	13.5 [-14.8]	19.6 [6.2]	51.6 [24.5]	14.1 [-13.1]
aza-heterocycle						
Dmap	9.9 [-3.9]	45.4 [18.7]	-3.0 [-31.0]	14.6 [0.9]	46.2 [19.5]	-2.6 [-30.0]
Py	15.4 [1.3]	47.3 [20.8]	-10.9 [-38.0]	20.1 [6.5]	48.5 [21.9]	-10.3 [-37.6]
Dbu	-1.0 [-16.6]	36.4 [8.3]	8.6 [-21.3]	6.7 [-7.3]	41.3 [14.1]	6.0 [-20.7]
Mtbd	0.3 [-15.4]	39.2 [11.8]	6.3 [-21.8]	9.6 [-3.3]	45.5 [18.8]	11.1 [-17.0]

Table S7: Free energies and enthalpies, ΔG [ΔH] in kcal mol⁻¹, for the [3 + 2] cycloaddition of the adducts (LB-**3** and LB-**3'**) and ethylene **2a**.

7 Cycloadditions with enone **2b**

The **Pph-3** adduct reacts with enone **2b** to form either α - or γ -[3 + 2] ylides, as shown in Figure S8. The γ -[3 + 2] cycloaddition (ΔG^\ddagger : 21.6 kcal mol⁻¹) requires a higher activation energy than the α -[3 + 2] addition (ΔG^\ddagger : 18.9 kcal mol⁻¹). The energy profiles of the PPh₃-catalyzed γ -[3 + 2] and γ -[2 + 4] cyclizations are shown in Figure S9. The γ -[3 + 2] cycloaddition starting with the *E*-type adduct **Pph-3'** is shown in Figure S10. The rate-determining step is the addition of PPh₃ to **1** in both γ -[3 + 2] cycloadditions starting from **Pph-3** and **Pph-3'**. The free energy of **Pph-ts3** is 24.2 kcal mol⁻¹, and thereby lower than that of **Pph-ts3'**, being 28.3 kcal mol⁻¹. Hence, the [3 + 2] cycloaddition starting from **Pph-3** dominates in kinetics.

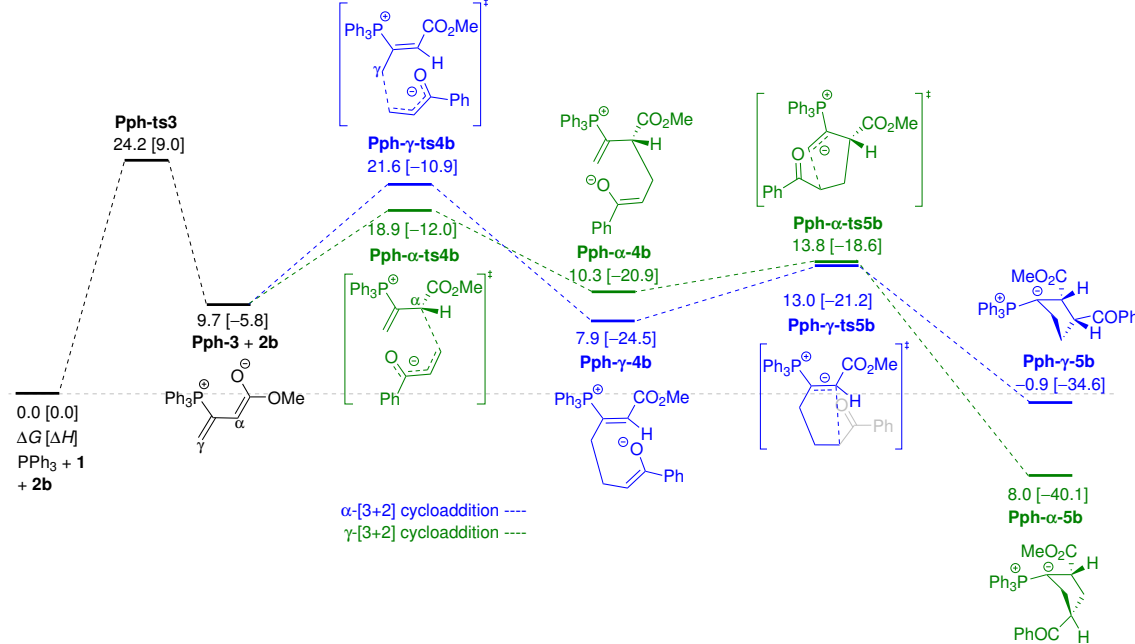


Figure S8: Energy profiles for the PPh₃-catalyzed α - and γ -[3 + 2] cycloadditions.

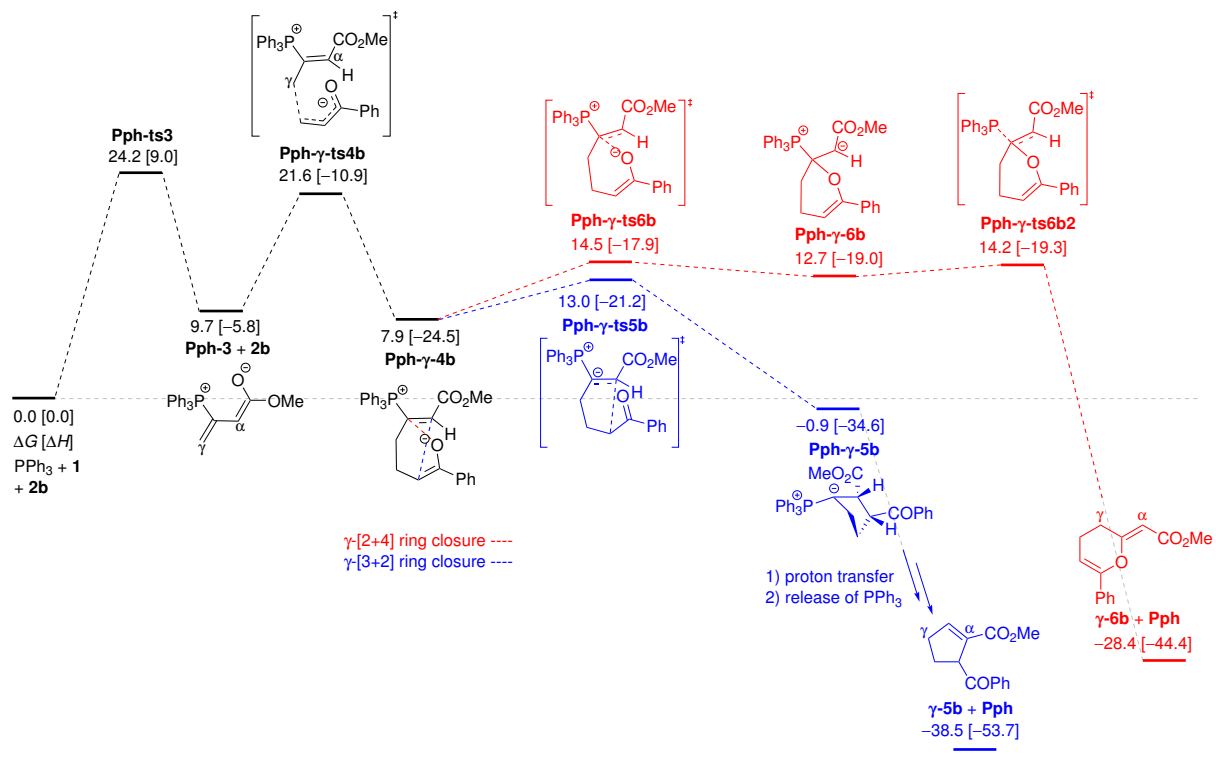


Figure S9: Energy profiles for the PPh_3 -catalyzed γ -[3 + 2] and γ -[2 + 4] cycloadditions.

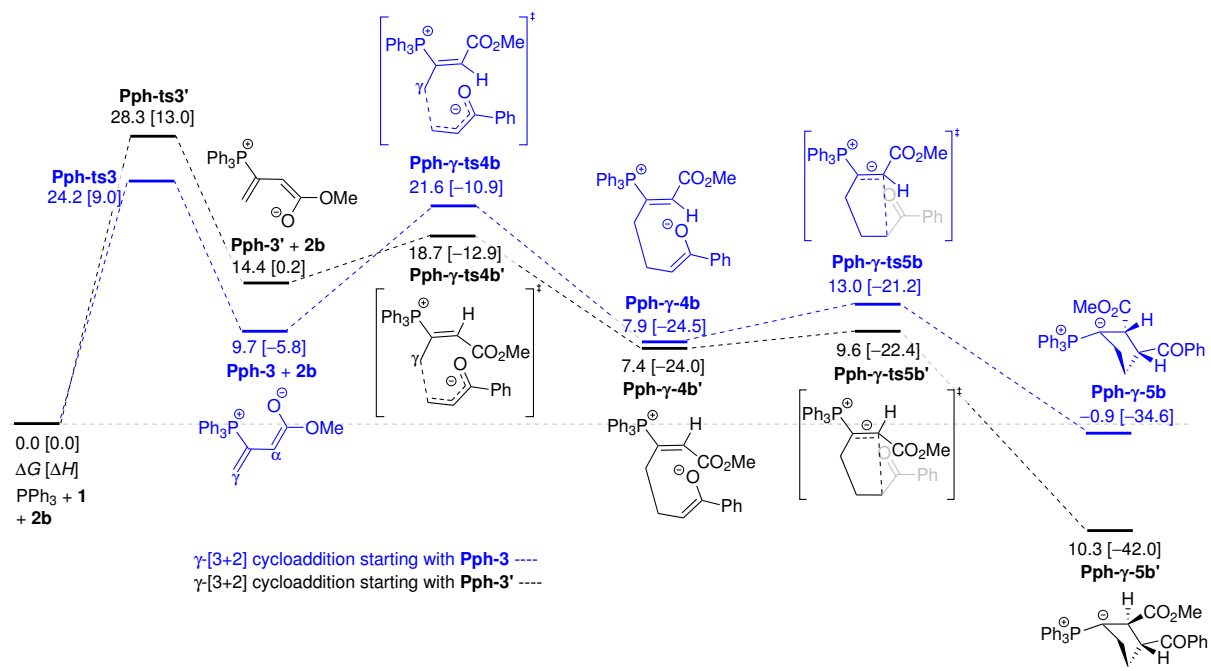


Figure S10: Energy profiles for the PPh_3 -catalyzed γ -[3 + 2] cycloadditions starting from **Pph-3** and **Pph-3'**.

Figure S11 shows the energy profiles for the γ -[2 + 4] cycloaddition starting from **Dabco-3** and **Dabco-3'**. The formation of **Dabco-3** is more favorable than that of **Dabco-3'**. However, the rate-determining step (rds) is the Michael addition of **Dabco-3/Dabco-3'** to **2b** in the overall reaction. The activation energy of **Dabco- γ -ts4b'**, being 23.8 kcal mol⁻¹, is lower than that of **Dabco- γ -ts4b**, being 25.1 kcal mol⁻¹. The calculations show that the formation of *E*-form dihydropyran products **γ -6b'** is kinetically more favorable, which agrees with experimental observation.^{1–4}

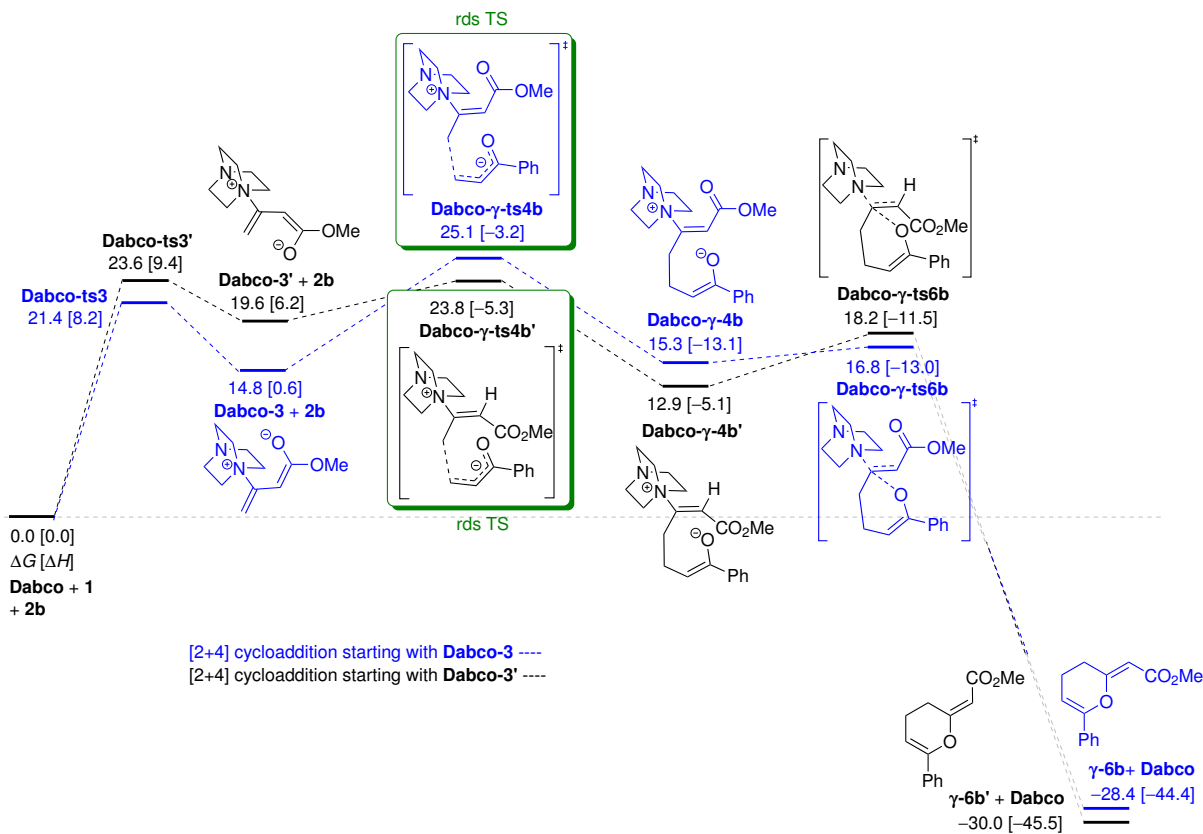


Figure S11: Energy profiles for the DABCO-catalyzed γ -[2 + 4] cycloadditions starting from **Dabco-3** and **Dabco-3'**.

8 Cycloadditions with ketone **2c**

Figure S12 shows the energy profiles and mechanism for the DABCO-catalyzed γ -[2 + 2], γ -[3 + 2] and γ -[2 + 2 + 2] cycloadditions of methyl allenate **1** and ketone **2c**. The highest barrier along the γ -[2 + 2] pathway is 26.2 kcal mol⁻¹. The γ -[2 + 2] pathway is kinetically more favorable than the γ -[3 + 2] and γ -[2 + 2 + 2] pathways with barriers of 35.2 and 28.3 kcal mol⁻¹.

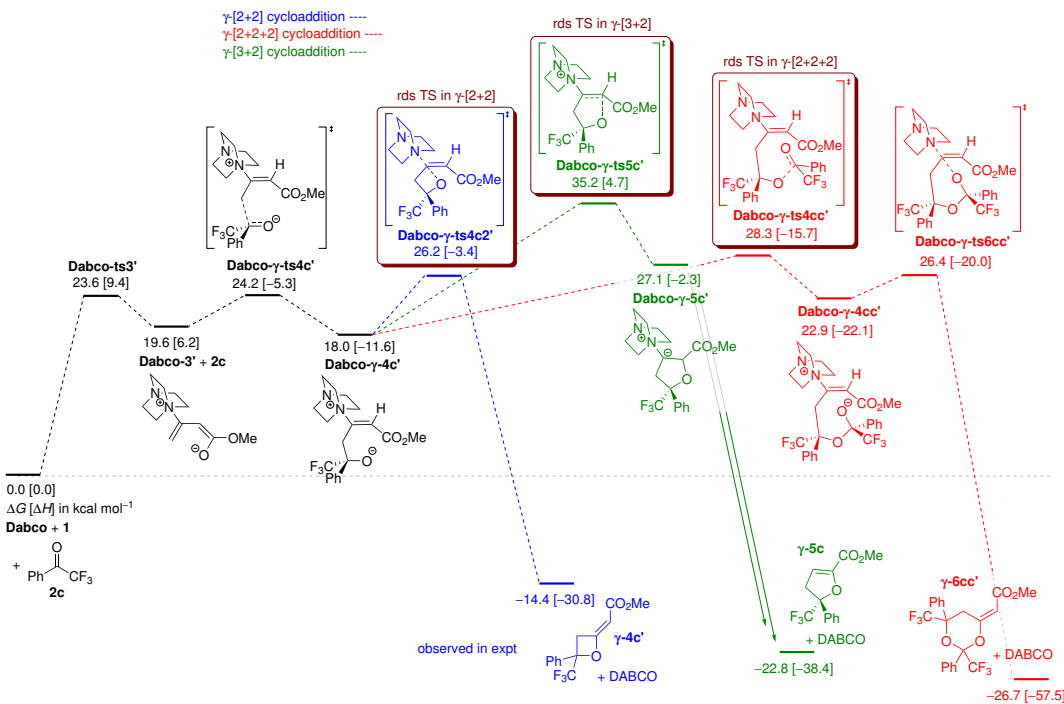


Figure S12: Energy profiles for the DABCO-catalyzed γ -[2 + 2], γ -[3 + 2] and γ -[2 + 2 + 2] cycloadditions of **1** and ketone **2c**.

Figure S13 shows the energy profiles and the mechanism for the NHC-catalyzed γ -[2 + 2], γ -[3 + 2] and γ -[2 + 2 + 2] cycloadditions of methyl allenate **1** and ketone **2c**. The highest barrier along the γ -[2 + 2] pathway is 5.3 kcal mol⁻¹ higher than that along the γ -[2 + 2 + 2] pathway. In regard of the stereochemistry of the [2 + 2 + 2] cycloaddition, the formation of the *trans*-product with the two trifluoromethyl groups on the same sides of the dioxane ring is kinetically more favorable than the formation of the [2 + 2 + 2] *cis*-product (Figure S14).

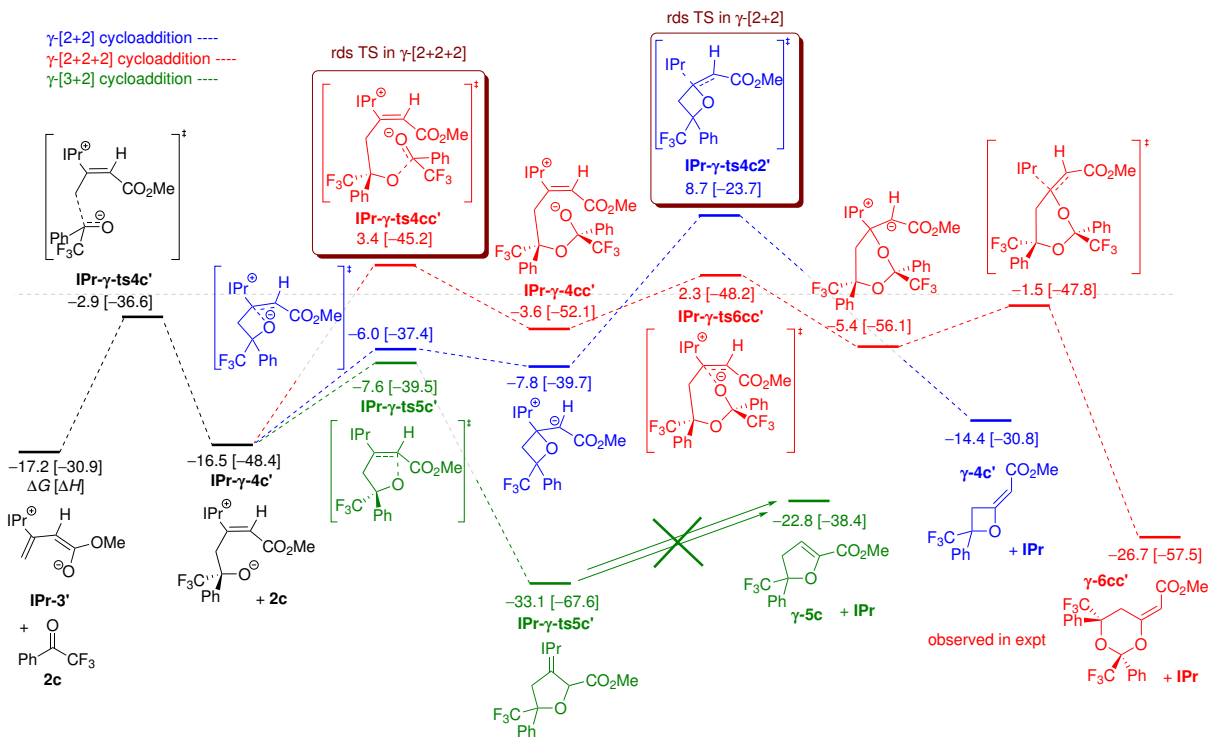


Figure S13: Energy profiles for the IPr-catalyzed γ -[2 + 2], γ -[3 + 2] and γ -[2 + 2 + 2] cycloadditions of **1** and ketone **2c**.

[2+2+2] cycloaddition yielding *trans*-products ----
 [2+2+2] cycloaddition yielding *cis*-products ----

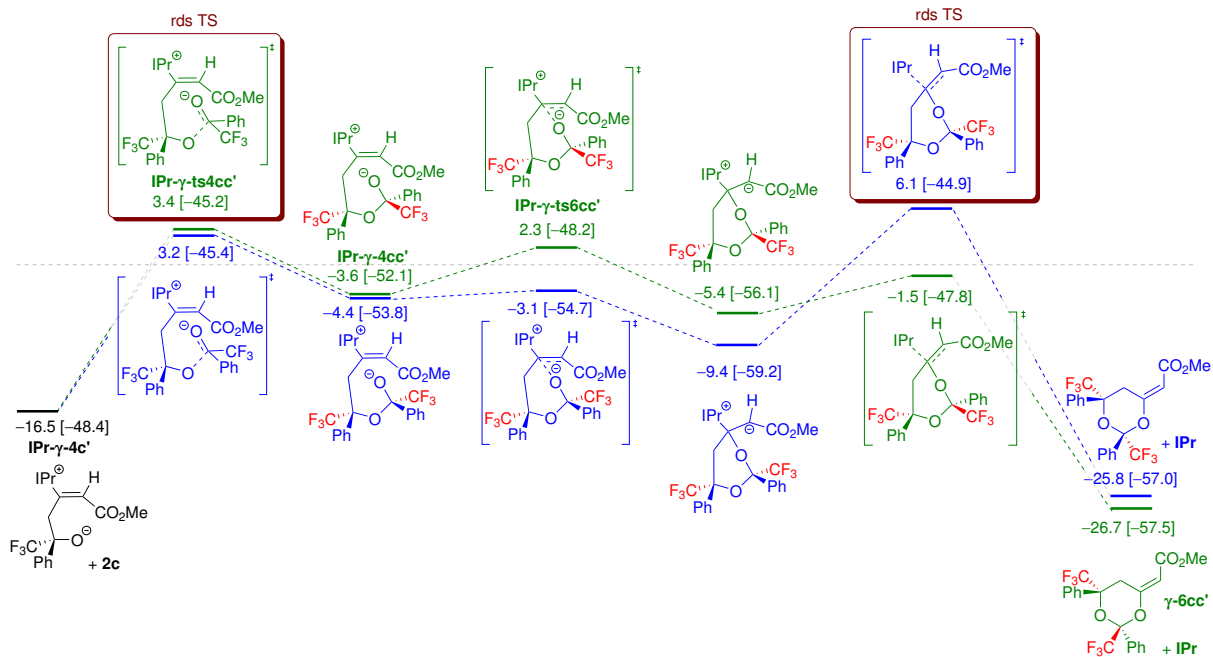


Figure S14: Energy profiles for the **IPr**-catalyzed γ -[2 + 2 + 2] cycloadditions, yielding *trans*- and *cis*-products.

Figure S15 shows the structure of **IPr- γ -5c'**. **IPr** and the trifluoromethyl group block the access to C _{α} and C _{β} which might aid the generally unfavorable [1,2] proton transfer.

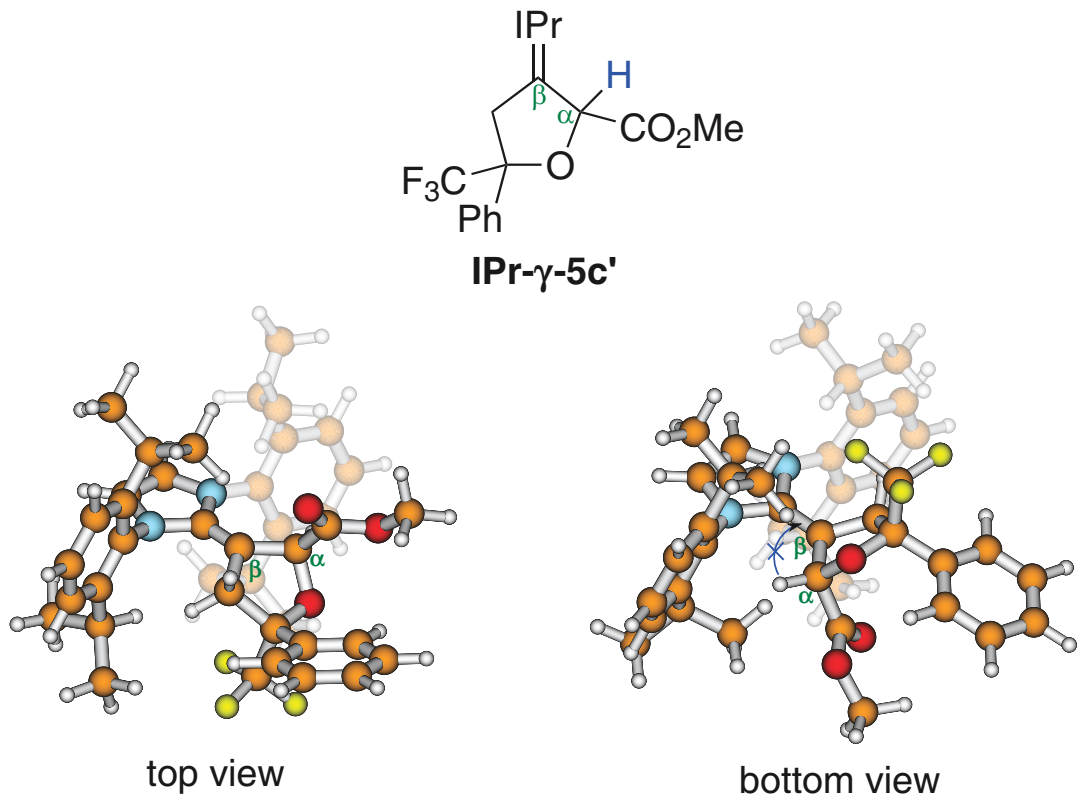


Figure S15: Geometry of **IPr- γ -5c'**.

Figure S16 shows the energy profiles and the mechanism for the PPh_3 -catalyzed γ -[2 + 2], γ -[3 + 2] and γ -[2 + 2 + 2] cycloadditions of methyl allenoate **1** and ketone **2c**. The cycloadditions start from the Z-type adduct, **Pph-3**. The highest barrier along the γ -[2 + 2 + 2] pathway is 28.9 kcal mol⁻¹, and the γ -[2 + 2 + 2] cycloaddition is hence the kinetically least favorable. The barriers for the γ -[3 + 2] and γ -[2 + 2] cycloadditions are similar. The formation of the γ -[3 + 2] products **γ-5c** is thermodynamically more favorable than that of the γ -[2 + 2] products **γ-4c**.

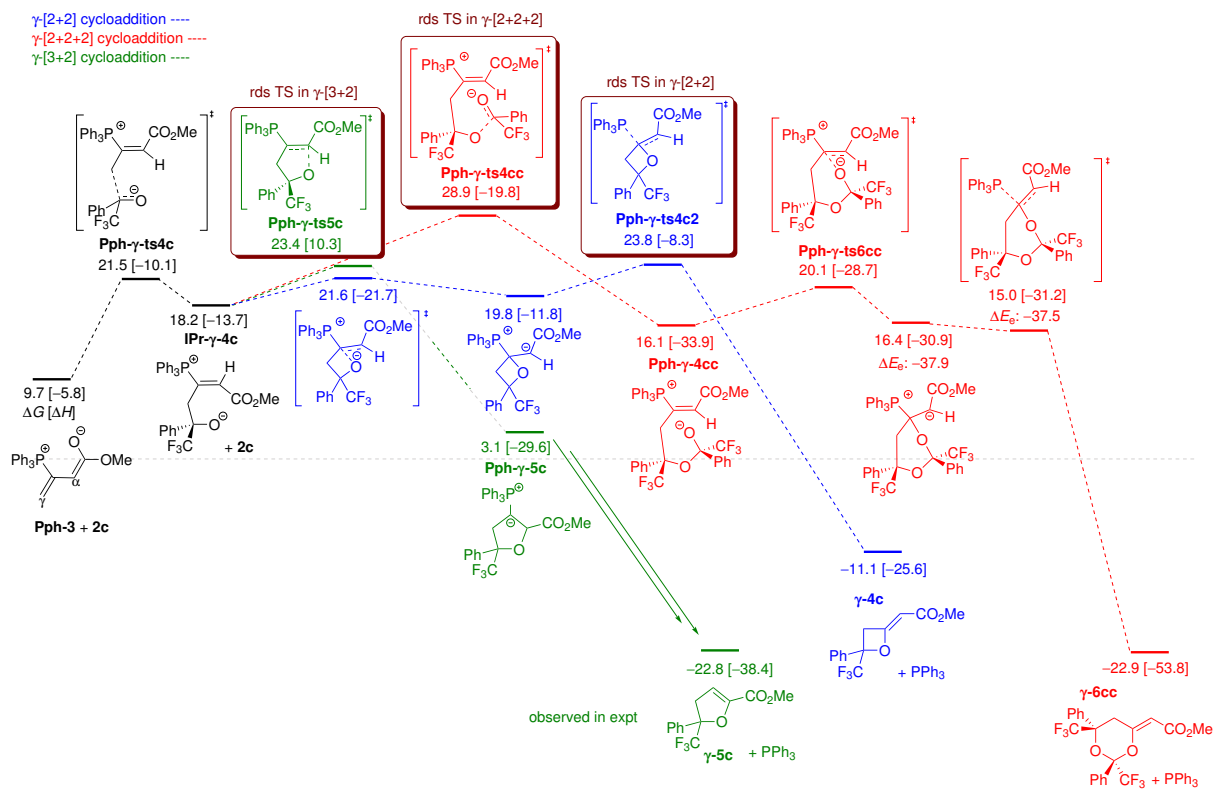


Figure S16: Energy profiles for the PPh_3 -catalyzed γ -[2 + 2], γ -[3 + 2] and γ -[2 + 2 + 2] cycloadditions of **1** and ketone **2c**.

C	2.270531	1.250205	0.043654	E(ele)	= -344.395985
H	3.340237	1.061740	-0.054622	E(ele+zpe)	= -344.295156
H	1.983837	1.962754	-0.737240	H	= -344.286572
H	2.086164	1.714037	1.023448	G	= -344.286549
C	2.270579	1.250188	0.043461	C	= -0.783242 -0.809215 -0.000911
H	2.086557	1.714000	1.023332	H	= -0.623234 -1.093450 -0.0001713
H	1.983301	1.962746	-0.737314	C	= -1.992032 -0.299139 -0.000102
H	3.340251	-1.061737	-0.055215	C	= -3.189211 0.213336 0.000877
				H	= -3.700476 0.439501 -0.930768
				H	= -3.699554 0.437702 0.933474
				C	= 0.414782 0.069457 -0.000530

Py

E(ele)	= -248.180089			
E(ele+zpe)	= -248.090298			
H	= -248.085096			
G	= -248.117692			
C	1.139571	-0.721256	-0.000001	
C	-1.139550	-0.721290	0.000001	
C	1.196383	0.671955	0.000001	
H	2.054596	-1.309255	0.000002	
C	-1.196403	0.671919	-0.000001	
H	-2.054557	-1.309317	-0.000001	
C	-0.000221	1.383282	0.000000	
H	2.155676	1.179725	0.000002	
H	-2.155711	1.179662	-0.000002	
N	0.000022	-1.416867	0.000000	
H	-0.000037	2.469601	0.000000	
			O	0.414642 1.276722 -0.000577

Dbu

E(ele)	= -461.888397		
E(ele+zpe)	= -461.639337		
H	= -461.628629		
G	= -461.674797		
C	2.133255	1.176928	0.339080
C	0.968804	1.581340	-0.609229
C	-0.322860	0.822912	-0.389755
C	1.929281	-0.126533	1.119123
C	1.890506	-1.379603	0.240124
C	0.971700	-1.191747	-0.979663
H	3.066815	1.119869	-0.234343
H	0.714499	2.633149	-0.10216
H	0.982562	-0.053611	1.580809
H	1.557319	-2.236324	0.836336
H	2.279793	1.982002	1.066279
H	1.271622	1.467383	-1.655644
H	2.711290	-0.231015	1.886524
H	2.899321	-1.620970	-0.120104
H	0.732882	-2.157824	-1.436182
H	1.466889	-0.08746	-0.74543
C	-2.580053	0.712811	0.163185
C	-2.298419	-0.654675	0.759217
C	-1.354054	-1.415421	-0.169315
H	-3.259235	1.283873	0.803260
H	-1.820634	-0.523653	1.742497
H	-3.218293	-1.241419	0.900223
H	-0.899306	-2.265005	0.357653
H	-1.904248	-1.821340	-1.030208
H	-3.080483	0.594800	-0.811277
N	-0.285864	-0.537475	-0.648483
N	-1.358249	1.491024	-0.009387

Mtbd

E(ele)	= -477.929684		
E(ele+zpe)	= -477.692770		
H	= -477.681858		
G	= -477.727838		
C	-2.328423	1.100614	0.201622
C	-0.054751	1.472866	-0.640825
C	-1.713005	1.238421	0.178151
C	-2.685580	-0.60942	-0.383532
C	-2.643216	1.145356	1.254831
H	-2.879216	1.894722	-0.315688
H	-1.884129	-2.276270	-0.258741
H	-1.842445	-1.374664	1.268950
H	-2.590135	0.238451	-1.475562
H	-3.716307	-0.538570	-0.138024
G	-2.327153	-0.093648	0.202478
C	2.016222	-1.500788	-0.272039
C	0.641128	-1.887564	0.236427
H	3.273980	0.255896	-0.220539
H	2.026609	-1.526778	-1.366968
H	2.767026	-2.204743	0.101189
H	0.325391	-2.850017	-0.182391
H	0.666392	-2.003380	1.336015
H	2.437295	-0.080233	1.304098
N	-0.348961	-0.894459	-0.151301
N	-0.912934	1.413302	0.124356
N	1.284557	0.822895	-0.231513
C	1.603069	2.227070	-0.038768
H	0.913061	2.842167	-0.614321
H	1.526548	2.528112	1.016878
H	2.625758	2.392893	-0.388998

s-trans methyl allenote 1

E(ele)	= -344.396253		
E(ele+zpe)	= -344.205473		
H	= -344.286854		
G	= -344.327977		
C	-0.856377	0.995681	-0.000050
H	-1.026279	2.068358	-0.000096
C	-1.855334	0.144463	0.000003
C	-2.851116	-0.695386	0.000050
H	-3.274034	-1.059942	0.932162
H	-3.274099	-1.059937	-0.932038
C	0.569529	0.583490	-0.000034
O	0.731472	-0.747932	-0.0000101
C	2.088119	-1.193026	0.000033
H	2.606357	-0.829384	-0.890377
H	2.606310	-0.828964	0.890295
H	2.038110	-2.280774	0.0000280
O	1.487868	1.370347	0.000072

s-cis methyl allenote 1

			Mfdb-3
C	0.191923	-0.499866	2.383498
C	1.660752	-0.249386	2.123629
H	-1.285851	-1.966625	1.775979
H	-0.404693	0.341503	2.008940
H	0.011923	-0.595488	3.486448
H	1.829950	0.707240	2.397427
H	2.289591	-0.927140	2.726574
H	0.347714	-2.627844	1.399045
N	1.980298	-0.442453	0.079667
N	0.006869	-1.607194	0.205263
C	-1.773934	-1.699911	-0.816164
C	-2.624406	0.833735	-0.212841
H	-3.478272	-1.196093	3.481888
C	-1.552823	-2.652274	1.700868
C	-2.311664	0.572906	-0.194281
O	-1.339647	1.105457	-0.713972
O	-3.221681	1.296904	0.511313
H	-2.278877	-2.795255	-2.496928
H	-0.680121	-3.292573	-1.661005
C	-2.971745	2.694743	0.566317
H	-2.013258	2.898164	0.533316
H	-2.952133	3.124504	-0.438822
H	-3.790497	3.119543	1.147269
			Dbu-3
E(ele)	-806.315710		
E(ele+zpe)	-805.960047		
H	-805.941926		
G	-806.004394		
C	-0.503420	-1.679967	-1.575121
C	-0.782214	-0.171380	-1.817542
C	-0.977372	0.586119	-0.530966
C	-1.075695	-2.276271	-0.283067
C	-2.558547	-2.114241	-0.090110
C	-3.057473	-0.664504	-0.290384
H	-0.871933	-2.231921	-2.448649
H	-0.045839	0.275285	-2.365905
H	-0.425958	-1.822028	0.559426
H	-2.848992	-2.451494	0.919822
H	0.583093	-1.810120	-1.545127
H	-1.678262	-0.033765	-2.430117
H	-0.829521	-3.343949	-0.258048
H	-3.144539	-2.748964	-0.789598
H	-3.987323	-0.472243	0.252133
H	-3.273577	-0.470732	-1.342854
C	-0.129830	0.272666	1.208559
C	-0.940748	1.207240	2.156858
C	-2.281800	0.880865	1.523185
H	0.908925	2.144162	1.538091
H	-0.381398	0.285997	2.341897
H	-1.090608	1.733534	3.102949
H	-2.813831	0.129183	2.114282
H	-2.921153	1.771468	1.452345
H	-0.540534	3.086044	1.118855
N	-2.083376	0.323023	0.182730
N	-0.090011	1.467282	-0.128836
C	1.125558	1.737480	-0.900882
C	2.193610	0.821178	-0.710653
H	3.095732	0.978687	-1.289515
C	1.058438	2.841271	-1.685516
C	2.188818	-0.244244	0.209096
O	1.307579	-0.576939	0.127766
O	3.344787	-0.991251	0.141904
H	1.918593	3.157837	-2.264947
H	0.149351	3.429092	-1.741218
C	3.415226	-2.079931	1.042972
H	3.324244	-1.743268	2.080110
H	2.622598	-2.809978	0.846143
H	4.392568	-2.537125	0.879635
			Mfdb-Is3
E(ele)	-822.317891		
E(ele+zpe)	-821.978092		
H	-821.959478		
G	-822.023226		
C	-0.121336	1.695896	1.940823
C	-1.103174	0.323234	0.212196
C	-0.296464	-0.732644	2.224623
C	-0.525153	0.597120	2.917291
H	-0.973911	1.781542	1.950450
H	-0.525296	2.664070	2.260845
H	-0.577813	-1.574798	2.864451
H	0.764543	-0.854894	1.947500
H	-1.584485	0.674603	3.187304
H	0.067074	0.670596	3.835358
C	-1.986336	-1.053746	-1.625349
C	-2.384540	-2.099127	-0.609048
C	-1.338589	-2.118428	0.495153
H	-2.786329	-0.914413	-2.359246
H	-3.364086	-1.850838	-0.176930
H	-2.451548	-3.084885	-1.071804
H	-1.649642	-2.769245	3.139614
H	-0.381161	-2.488845	0.096625
H	-1.074625	-1.355751	-2.158680
N	-1.147795	-0.781186	1.043653
N	-0.544351	1.467200	0.563032
N	-1.769974	0.233408	-0.975019
C	1.049837	2.016097	-0.549598
C	2.085416	1.164635	-0.298871
H	2.955671	1.526271	0.238902
C	0.688498	3.168203	-1.082272
C	1.996085	-0.238238	-0.583690
O	1.045304	-0.828278	-1.091202
O	3.110931	-0.915435	-0.193160
H	1.329909	3.608178	-1.841783
H	-0.217884	3.687317	-0.797010
C	3.105119	-2.309310	-0.464311
H	2.296071	-2.808645	0.077618
H	2.979367	-2.496012	-1.534279
H	4.071236	-2.681398	-0.123153
C	-1.861792	1.380587	-1.856883
H	-1.885751	2.291531	-1.261608
H	-1.014382	1.429902	-2.550513
H	-2.791234	1.293799	-2.429006


```

H      0.122511   -2.709809  -1.085895
H      -1.330197   -1.100637  -2.259908
H      -2.155932   -2.659472  -0.564529
H      -3.624284   -0.678426  -1.574253
H      -3.605915   -2.021948  -0.411936
H      -1.207044   -3.101020  -0.009082
H      -2.528991   -0.314267  0.154956
N      -0.412653   -1.261472  0.277624
N      -0.1015358  -1.158132  0.62901
C      1.675973   -0.233842  -0.225260
H      1.119137   -0.272605  -1.006383
C      1.417727   -1.969348  1.631499
C      3.065206   0.022347  -0.101851
O      3.851061   -0.476178  0.701888
O      3.505936   0.961512  -1.015158
H      2.461748   -2.003176  1.912187
H      0.694266   -2.586693  2.154514
C      4.888116   1.259313  -0.934596
H      5.149661   1.652747  0.052555
H      5.494245   0.367407  -1.121330
H      5.077115   2.011081  -1.703144

```

Mtdb-ts3'

```

E(ele)      = -822.313257
E(ele+zpe)  = -821.973741
H      = -821.954785
G      = -822.020377
C      -2.520862   -1.520654  -0.431796
C      -1.094086   0.185767  0.502294
C      -2.501425   0.738441  -1.396841
C      -3.406474   -0.368059  -0.884009
H      -2.103060   -2.019080  -1.318601
H      -3.107234   -2.275393  0.105148
H      -3.078528   1.619236  -1.696894
H      -1.928593   0.397233  -2.273703
H      -4.004606   0.014485  -0.048754
H      -4.096738   -0.617923  -1.670686
C      0.666738   1.779293  1.282226
C      -0.260547   2.807354  0.163077
C      -0.958819   2.449089  -0.503077
H      1.012564   2.018799  2.268891
H      -1.051289   3.122399  1.538570
H      0.239375   3.804064  0.600566
H      -1.729147   3.164334  -0.811910
H      -0.236480   2.303131  -1.313982
H      1.459639   1.618211  0.606503
H      -1.603737   1.153226  -0.325873
N      -1.424027   -1.093136  0.429929
N      -0.160634   0.546272  1.414830
C      -0.162119   -2.065519  -0.106409
C      0.918143   -1.310411  0.969045
H      0.513778   -1.009810  -1.932666
C      0.050205   -3.226065  0.513135
C      2.135825   -0.688250  -0.540215
O      2.747161   -0.845091  0.510927
O      2.604749   0.194935  -1.484427
H      0.728712   -4.027291  0.234173
H      -0.680157   -3.400416  1.295201
C      3.878184   0.754245  -1.198797
H      3.853714   1.343668  -0.277065
H      4.630677   -0.030999  -1.084929
H      4.120924   1.391515  -2.050055
C      0.297717   -0.393342  2.433373
H      -0.479749   -1.135272  2.608692
H      1.223128   -0.890537  2.421964
H      0.477002   0.174996  3.351833

```

Mtdb-3'

```

E(ele)      = -822.335268
E(ele+zpe)  = -821.993063
H      = -821.973996
G      = -822.040534
C      1.139745   2.444616  -0.045529
C      1.258114   -0.004615  0.254744
C      2.493205   1.043489  -1.536729
C      2.513045   2.010369  -0.593311
H      0.418712   2.832057  -0.775222
H      1.160934   3.138630  0.799472
H      3.447827   0.875869  -2.041528
H      1.704250   1.100730  -2.298743
H      3.299132   2.205683  0.074507
H      2.730358   3.188999  -1.288525
C      1.327637   -2.394331  0.432125
C      2.825271   -2.353183  0.172184
C      3.115871   -1.267720  -0.843886
H      1.066909   -3.151935  1.172806
H      3.341056   -2.159970  1.116889
H      3.187675   -3.322113  -0.212548
H      4.162671   -0.945915  -0.784984
H      2.941540   -1.641803  1.861215
H      0.761972   -2.610903  -0.485110
N      2.257700   -0.097910  -0.655135
N      0.608548   1.157020  0.426984
N      0.931311   -1.096898  0.966607
C      -0.857502   1.144125  0.607066
C      -1.501194   0.290015  -0.328305
H      -0.925775   -0.158457  -1.132333
C      -1.336906   1.955983  1.581971
C      -2.891082   0.032533  -0.275716
O      -3.713584   0.469216  0.529998
O      -3.297659   -0.837653  -1.275543
H      -2.404480   2.061433  1.717628
H      -0.656214   2.482218  2.244744
C      -4.686051   -1.111171  -1.289526
H      -5.009611   -1.566798  -0.348428
H      -5.266740   -0.196228  -1.444690
H      -4.846860   -1.803519  -2.118417
C      0.067264   -1.063764  2.143441
H      0.155815   -0.098235  2.637895
H      -0.981399   -1.216413  1.866405
H      0.408324   -1.851389  2.820672

```



```

C      5.257457   -1.550432   -1.435407
H      4.206968    0.124011   -0.594108
C      5.245151   -2.028983   -1.36913
H      4.224396   -4.779870   -1.28852
H      6.066686   -0.938104   -1.821383
H      6.080930   -3.395873   -2.180471

```

75c

```

E(ele)      -1026.844345
E(ele+zpe)  -1026.619735
H           -1026.602270
G           -1026.665528
C      -1.708644   0.090044   0.711650
C      0.135150   1.125078   1.631418
C      -1.318384   0.773096   1.784612
C      0.455430   0.540852   0.222222
H      0.312397   2.205373   1.675756
C      -3.064005   -0.458122   0.452907
O      -3.981795   -0.331905   1.229023
O      -3.140419   -1.092966   -0.717222
C      -4.426951   -1.634077   -1.029058
H      -4.718404   -2.369716   -0.275929
H      -5.172075   -0.836104   -1.061488
H      -4.316630   -2.101082   -2.005958
H      0.755133    0.654478   2.401377
O      -0.735954   -0.115331   -0.231615
C      0.672306    1.684732   -0.779123
C      1.629519   -0.419641   0.185196
C      2.828748   -0.078971   0.816996
C      1.528637   -1.633679   -0.494854
C      3.915022   -0.948184   0.774937
H      2.920035   0.869823   1.340350
C      2.616511   -2.504591   -0.530007
H      0.596785   -1.892276   -0.986529
C      3.810032   -2.165231   0.102592
H      4.842515   -0.381942   1.269308
H      2.564656   -3.631988   -1.055340
H      4.656226   -2.845361   0.073425
F      -0.388164   2.507749   -0.800854
F      1.743011   2.425110   -0.437971
F      0.864136   1.235678   -2.021119
H      -1.950315   1.017839   2.626996

```


Acknowledgement

This work is supported by the National Science Council of the Republic of China under Grant NSC 100-2113-M-007-008-MY3. Timm Lankau acknowledges a university research associateship from the National Tsing Hua University.

References

- (1) Pei, C.-K.; Wu, L.; Lian, Z.; Shi, M. *Org. Biomol. Chem.* **2012**, *10*, 171–80.
- (2) Wang, X.; Fang, T.; Tong, X. *Angew. Chem. Int. Ed.* **2011**, *50*, 5361–4.
- (3) Ashtekar, K. D.; Staples, R. J.; Borhan, B. *Org. Lett.* **2011**, *13*, 5732–5.
- (4) Chen, X.-y.; Wen, M.-w.; Ye, S.; Wang, Z.-x. *Org. Lett.* **2011**, *13*, 1138–41.